J Therm Anal Calorim (2012) 107:955–962
DOI 10.1007/s10973-011-1611-9

Synthesis of bismuth mixed oxide by thermal decomposition of a coprecipitate precursor

Abdellah Bahmani · Mayouf Sellami · Noureddine Bettahar

Received: 5 March 2011 / Accepted: 19 April 2011 / Published online: 5 May 2011

Abstract Bismuth mixed oxide powders were prepared by oxalate coprecipitation process. The thermal decomposition behaviour of the coprecipitate precursors has been followed by thermal analysis (TG-DTA) and FTIR spectroscopy. During the decomposition of the precursor, several intermediates species were detected and a mechanism of formation of mixed oxide by this method is proposed. After the thermal treatment, the precursor obtained of suggested formula $Ca_3[Bi_6O_6(C_2O_4)_4(OH)_3NO_3]0.5H_2O$, has led to the formation of $CaBi_2O_4$ at shorter reaction time than the traditional ceramic method. In order to consolidate the results, the coprecipitation in absence of oxalic precipitant under the same conditions was examined. XRD and scanning electron spectroscopy were used to study particles sizes and morphology.

Keywords Bismuth oxides · Coprecipitation · Oxalate · Thermal analysis · X-ray diffraction

Introduction

At present great interest is devoted to bismuth-based oxides because they present a wide variety of materials where bismuth is found either as an essential component or as an additive. So far these materials have been demonstrated to be potentially useful as superconductors [1, 2], oxidation catalysts [3, 4], photocatalysts, [5, 6], pigments [7, 8], scintillators [9, 10], sensors [11], high temperature electrolytes [12, 13] and next generation data storage materials [14].

The Bi_2O_3–CaO phase diagrams have been investigated over the whole composition range [15–17]. The system has been reviewed and optimised thermodynamic descriptions were presented by Hallstedt et al. [18]. The mixed oxides compounds were prepared by the authors through a solid-state route by firing mixtures of oxides and carbonates of the constituent elements at high temperatures with intermittent grinding.

In addition to this ceramic technique, the wet chemical methods of preparation are becoming increasingly important. Among the chemical methods, the chemical coprecipitation technique is widely investigated for ceramic powder preparation. These chemical methods have important advantages, such as the production of more homogeneous powders, good stoichoimetric control and short thermal treatment.

Considerable efforts have been devoted in recent years to study the preparation of oxalates of metallic ions or mixture of metallic ions and their decomposition to obtain the correspondent oxides [19–30]. In these former studies, the oxalate ion was found to have a multidentate character; it can form with metal centres chains, layers or three-dimensional networks.

The characteristics of Bi and oxalates provide a wide-ranging potential for the synthesis of new compounds that may be useful in technology application. However, the oxalate coprecipitation in the synthesis of Bi-based systems presents different opinions referring to some major aspects, such as the pH of coprecipitation and the precipitating agent [26–35].

Therefore exact knowledge of the relationship between synthesis method, processing condition, microstructure and

A. Bahmani (✉) · M. Sellami · N. Bettahar
Laboratoire de Physico-Chimie des Matériaux-Catalyse et Environnement, Faculté des Sciences, Département de Chimie, Université des Sciences et de la Technologie d'Oran, B.P. 1505, El-Mnaouer, 31000 Oran, Algeria
e-mail: bahmani_abdallah@yahoo.fr

grain size of mixed oxide powder is required. Our work is focussed on the comparison and optimization of synthesis method.

The present article describes the preparation of bismuth calcium oxide by the oxalate and/or hydroxide coprecipitation processes and subsequent calcinations at high temperature and reports new results of synthesis.

Experimental

Materials

In order to prepare the calcium bismuth oxides, the metal elements are introduced in the form of nitrate salts, $Bi(NO_3)_2{\cdot}5H_2O$, $Ca(NO_3)_2{\cdot}4H_2O$. The precipitating agents used are: oxalic acid $(H_2C_2O_4){\cdot}2H_2O$ and diethylamine $(CH_3–CH_2)_2NH$. All the reagents used were of analytical grade materials AR Labosi.

Experimental procedures

The preparation of bismuth calcium oxides were performed in two steps: The preparation of the precursors then their calcinations at various temperatures to obtain desired oxides. In this work, two different methods of synthesis based on chemical coprecipitation were adopted to prepare the precursors:

Method I: based on obtaining a precipitate from oxalates.

Method II: based on obtaining a precipitate from hydroxides, at the same conditions in absence of oxalic precipitant.

The homogeneous precursor was performed by the following procedure: The nitrate of bismuth dissolved in concentrated nitric acid and aqueous solution of calcium nitrate were mixed in required stoichoimetric ratio (2:1, respectively). The aqueous solutions of nitrates, oxalic acid and diethylamine were added dropwise individually and simultaneously to 100 mL of distilled water, with continuous magnetic stirring. The pH maintained constant at 11. Finally, the fine oxalate (or hydroxide) precipitates thus obtained were filtered and washed with bidistilled water at the same pH. The samples were then dried gradually in an oven up to 80 °C for about 18 h. To obtain mixed oxides, the above mentioned precursors were calcined gradually at various temperatures 650, 700 and 800 °C according to the case, for 6 h.

Characterisation of powder

The produced precursors have been chemically analysed and their thermal decomposition and behaviour were studied by classical thermogravimetry and differential thermal analysis (TG-DTA, Setaram TGDTA 92) in the temperature range 30–800 °C at a heating rate of 10 °C min^{-1}, under an ambient atmosphere.

The intermediate and final compounds of thermal decomposition of the precursors are studied by means of Fourier transform infrared spectrophotometer (FTIR, Nicolet 630) in the 4000–350 cm^{-1} region.

X-ray powder diffraction (XRD) analysis of the calcined precursors obtained by the two methods, were carried out on Philips PW 1710 Diffractometer, employing a scanning rate of 0.02° and a speed of 1.2° min^{-1}, in the 2θ range from 10° to 70°.

The morphology and size of the synthesised powders were studied by scanning electron microscopy (SEM, JSM-5610LV).

Results and discussion

Chemical analysis of the two precursors is realised by colorimetry with thiourea for bismuth and by titration with EDTA for calcium and with $KMnO_4$ for oxalate ion. All the results are reported in Table 1 for the two obtained unknown precursors. The given oxalate percentages correspond to the samples of the oxalate precursor calcined to the indicated temperatures.

A chemical formula is proposed for each compound, based on these results and confirmed by FTIR and TG-DTA measurements and complete XRD studies, as well as on the bibliographical data.

The thermal behaviour of the oxalate and hydroxide obtained by the coprecipitation processes are shown in

Table 1 Chemical analysis of obtained precursors

Precursors	Bi/wt%		Ca/wt%		C_2O_4/wt%							
	Ambient *t*		Ambient *t*		Ambient *t*		290 °C		390 °C		490 °C	
	Exp.	Theor.	Exp.	Theor.	Exp.	Theor.	Exp.	Theor.	Exp.	Theor.	Exp.	Theor.
Oxalate	63.7	64.5	6.0	6.2	17.8	18.1	12.3	12.1	7.4	7.7	0	0
Hydroxide	86.9	–	1.0	–								

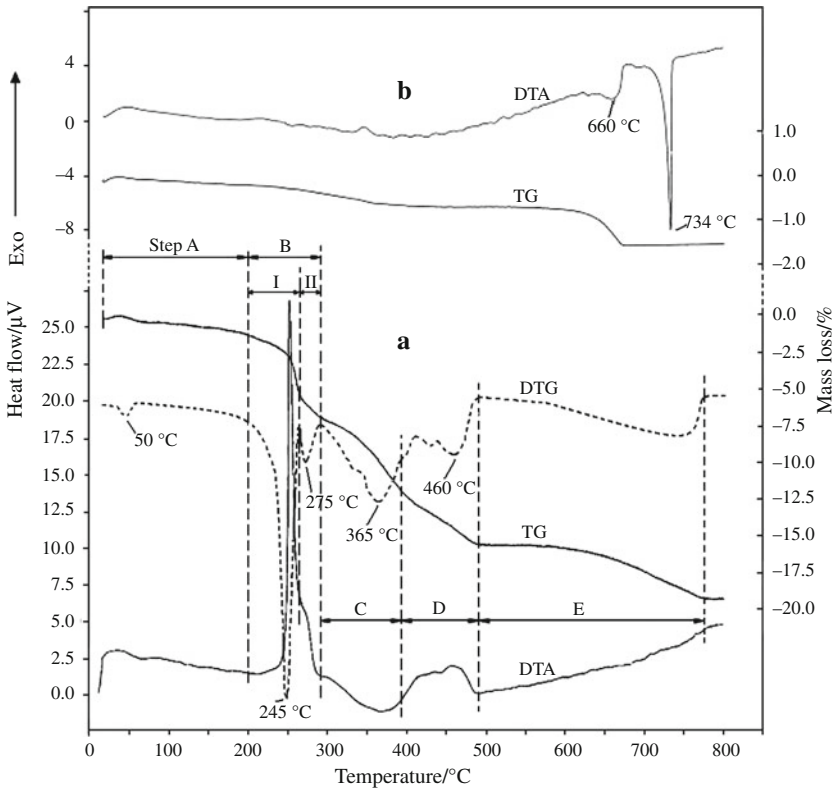

Fig. 1 TG, DTG and DTA curves of the oxalate (*a*) and the hydroxide (*b*) precursors in air

Table 2 Thermal analysis data for the decomposition of precursors (after drying at 80 °C)

Temperature range/°C	Weight loss/%		Species lost	Thermal effects	Phase composition
	Exp.	Theor.			
Oxalate precursor $Ca_3[Bi_6O_6(C_2O_4)_4(OH)_3NO_3]0.5H_2O$					
40–200	0.5	0.46	H_2O	Endoth./50 °C	$Ca_3Bi_6O_6(C_2O_4)_4(OH)_3NO_3$
200–260	4.8	4.63	CO_2, NO_2	Exoth./245 °C	$Ca_{1.5}(BiO)_4O(C_2O_4)(OH)_3 + (BiO)_2(C_2O_4) + 1.5Ca(C_2O_4)$
260–290	1.5	1.44	CO	Exoth./275 °C	$Ca_{1.5}(BiO)_4O(C_2O_4)(OH)_3 + (BiO)_2(CO_3) + 1.5Ca(C_2O_4)$
290–390	5.0	5.09	CO, CO_2, H_2O	Endoth.	$Bi_2O_3 + CaO + (BiO)_2CO_3 + Ca(C_2O_4) + (CO_2)$adsorb
390–490	4.3	4.42	CO, CO_2	Exoth.	$CaCO_3 + (Bi_2O_3 + CaO) + Bi_{1.6}Ca_{0.4}O_{2.6} + (CO_2)$adsorb
490–770	3.3	3.39	CO_2	Exoth.	$CaBi_2O_4$
Hydroxide precursor $(1 - y - z)Bi_2O_3 + 2yBiO(OH) + 2zBiO(NO_3) + xCaCO_3$					
200–400	0.7	–	H_2O, NO_2	Endoth.	α-$Bi_2O_3 + xCaCO_3$
620–680	0.9	–	xCO2	Endoth./660 °C	α-$Bi_2O_3 + \beta_2Bi_{2(1-x)}Ca_{(x)}O_{(3-2x)}$
690–745	–	–	–	Endoth./734 °C	δ-$Bi_2O_3 + \beta_1Bi_{2(1-x)}Ca_{(x)}O_{(3-2x)}$

Fig. 1. The endothermic and exothermic behaviours observed in the differential thermal analysis curve with their temperature range and corresponding mass losses in thermogravimetry at final temperature and successive decomposition steps in differential thermogravimetry are given in Table 2.

Thermal decomposition of oxalate precursor

The TG curve of oxalate precursor shows that the total mass loss of the precipitate is 19.4% and occurs in five steps (A → E), indicating that the precipitate comprises various anions in addition to oxalates. Therefore, it can be concluded that the precipitate may contain other anions in addition to oxalates. These findings are contrary to other authors [26–28].

The first step (A) of the TG profile, with the slight mass loss of about 0.5% at a range of 35–75 °C might be attributed to the release of the absorbed water. The IR spectrum (Fig. 2) recorded for the sample obtained at the end of this stage shows absorption bands at 1600, 1385 and 1315 cm^{-1} corresponding to different modes of vibration

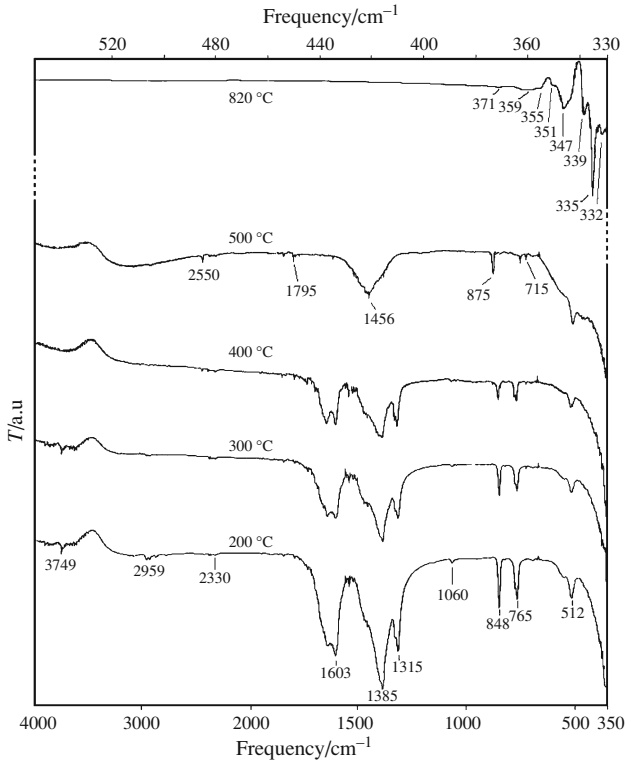

Fig. 2 IRTF spectra of the oxalate precursor heat-treated at various temperatures

of oxalate group [36, 37]. The two strong absorption bands appearing in the vicinities of 1385 and 1600 cm^{-1} can be attributed to the symmetric and asymmetric vibration of the carbonyl groups, while the absorption at 1315 cm^{-1} corresponds to ν(C–O). The sharp band appearing at the 774 cm^{-1} is characteristic of oxalates metallic species ν(C–O–M). The two broad bands around 3000 and 3750 cm^{-1} correspond to the structural OH groups' vibrations which are due to the presence of hydroxides.

The well-resolved band at 1603 cm^{-1} due to ν(NO) vibration indicates the presence of bidentate nitrates in the precursor. Other bands of the NO_3 group occur approximately at 1385, 1322, 1060, 840 and 760 cm^{-1} can be assigned to $\nu(NO_2)$, $\nu(NO_2)$, ν(NO), $\nu(NO_3)$ and $\nu(NO_3)$ bands, respectively, as a result of the employed reagents. It should be mentioned that the band at 1603 cm^{-1} is possibly overlapped with the ν(C–O) vibration of the carboxylate group present in the oxalate. The spectrum indicates an oxalate coordination to the Bi^{3+} and Ca^{2+} in the precursor, while the nature of such coordination is not yet clear.

Further, the wide absorption band located at 512 cm^{-1} is ascribed to the metal–oxygen–metal bond. Occlusion or sorption of CO_2 in the solid is certainly responsible for the band observed around 2330 cm^{-1} (ν_3 CO_2) [38, 39].

The second step B showed a strong exothermic peak in DTA with less drastic mass loss is observed in the temperature range 200–300 °C which corresponds to the reaction which is a result of a thermally induced redox reaction between the two anions present in the precipitate, where oxalate acts as a reductant and nitrate as an oxidant.

The IR spectrum (Fig. 2) of the product obtained at the decomposition stage end (step B) shows a reduction in the intensities of the oxalate and nitrate bands and an increase in those being in the oxide region of the IR spectrum. Thus, the oxalate at this stage has decomposed partially, as shown in the decomposition scheme. This degradation step is divided into two parts. The first part in the temperature range 200–260 °C, the mass loss observed for this stage (4.8%) tallies with the calculated loss of 4.63% for the removal of 1 mol of the nitrate of the empirical formula suggested of the precursor and one mole of CO_2, while the second part in the temperature range 260–290 °C with a mass loss of 1.5% corresponds to the loss of 1 mol of CO resulting from the degradation of 1 mol of oxalate.

The third step (C) is endothermic as indicated by the DTA curve in the temperature range 290–390 °C. The IR spectrum of the product obtained at the end of this stage shows another reduction in the intensity of oxalate bands with the carbonate bands still appearing at 1450 cm^{-1}, and at 1385 cm^{-1}. The hydroxyl stretching band at 3770 cm^{-1} was found to be absent at this stage indicating a loss of OH^- group from the precursor molecule.

The observed mass loss of 5.0% obtained during this stage is in agreement with the calculated loss of 5.09% and corresponds to the release of 1 mol of CO, CO_2 and a loss of 1.5 mol of water. This weak and irregular endothermic behaviour is due to the overlapping of the endothermic effect of the dehydration which surpasses the exothermic effect of oxidation of CO to CO_2.

In the fourth decomposition step (D), in the temperature range 390–490 °C, further decomposition of the remaining oxalates and the intermediate compounds takes place. The IR shows that characteristic bands of the oxalate group vanished and that broad carbonate band at 1456 cm^{-1} reveals that there is still some unreacted carbonate.

The oxide bands obtained in the spectrum are now much stronger, which is due to the formation of oxide phase at the end of this stage.

Also in this case, the irregular exothermic conduct of the DTA curve is due to the overlapping of the exothermic effect of the oxidation of CO to CO_2, which exceeds the endothermic effect of decomposition of the intermediates $Ca(C_2O_4)$ and $(BiO)_2CO_3$.

The last stage (E) which the slow variation of the shapes of the DTA and TG curves shows the progressive decomposition of remaining carbonates. IR spectrum of the resulted product shows the complete degradation of the

precursor and the intermediates and the formation of mixed oxide, which was also noticed in the XRD pattern.

By comparing with the curves of TG and DTA of the pure oxalate of Bi or Ca [21, 29], it is noted that the curves of TG and DTA of the precursor do not present any behaviour of degradation of bismuth oxalate compound, on the other hand, the calcium oxalate and its decomposition product, the calcium carbonate, are probably expected like intermediates.

Oxides formation process

To account for the intermediate species formed during the thermal treatment in air of the precursors, X-ray diffractograms of the inorganic residues formed at different temperatures 650 and 800 °C were collected.

According to the studies of FTIR and XRD, it was revealed that a thermal treatment of the precursor at 650 °C (Fig. 3) yielded a mixture of bismuth mixed oxide $CaBi_2O_4$ (JCPDS No. 48-0216), a phase identified as a solid solution of formula $Bi_{1.6}Ca_{0.4}O_{2.8}$ (JCPDS No. 41-0309) and a calcium carbonate $CaCO_3$ (JCPDS No. 86-2339). Some diffraction peaks detected in this residue were broad, which is indicative of a poor crystallinity. As the calcined temperature increased $CaCO_3$ reacted with the formed solid solution into $CaBi_2O_4$ which is the only phase identified finally at 800 °C and all the 2θ-line patterns match with reported values (JCPDS No. 48-0216).

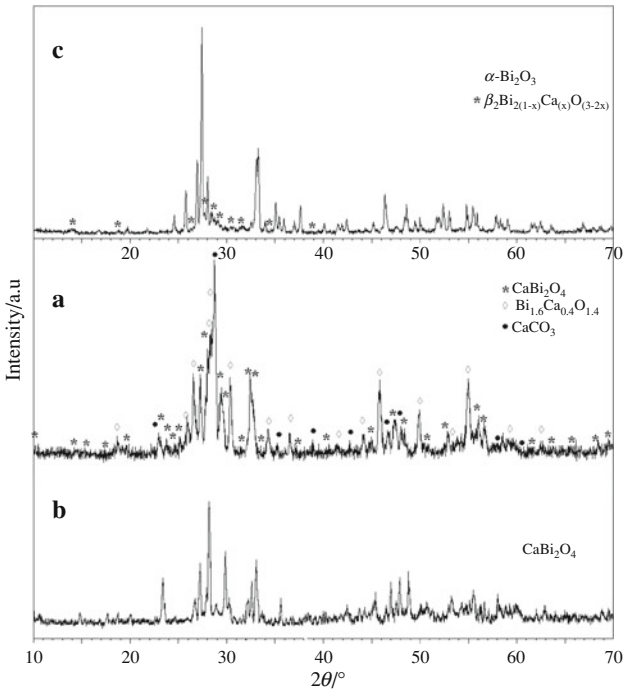

Fig. 3 XRD patterns of oxalate precursors powders (annealed at 650 °C (*a*), 800 °C (*b*)) and of hydroxide (at 700 °C (*c*))

The following bibliographical data and the investigation on the reactions of thermal decomposition of the oxalate precursor lead to the clarification of the important steps of the thermal decomposition in air of the precursor and the determination of the different corresponding intermediate products.

The bismuth(III) forms stable homo- and heterometallic complexes with a large number of ligands [40–42] and it readily hydrolyzes in aqueous solutions (pKa = 1.51) and has a high affinity to both oxygen and nitrogen ligands [43, 44]. Mehring et al. have recently reported several polynuclear bismuth oxo clusters which might be described in terms of assemblies of the hexanuclear motif [45, 46].

It is well established that the aqueous chemistry of bismuth is dominated by hexanuclear cations of the type $[Bi_6O_{4+x}(OH)_{4-x}]^{(6-x)+}$ [47], where the hexanuclear $[Bi_6O_8]^{2+}$ motif is found to be the central structural unit in a large variety of compounds such as bismuth oxo hydroxo nitrates [48–52] and bismuth oxo citrate [53, 54]. The tetranuclear building block can be built from the hexanuclear core structure by removal of two bismuth atoms and the attached oxygen atoms from the latter. $(Bi_2O_2)^{2+}$ layers represent a characteristic structural element of various bismuth compounds, of which some principal representative structures are as follows: The Sillèn phases [55], the Aurivillius phases $(Bi_2O_2)^{2+}(A_{n-1}B_nO_{3-n})^{2+}$ [56], the basic bismuth carbonates $(BiO)_2CO_3$ [57] and $(BiO)_4(OH)_2CO_3$ [58], bismuth oxysalts of carbonic acids with the general formula BiO(OOCR) [59].

Scheme 1 represents the probable course of the decomposition reactions of the precursor in the range of temperatures from 20 to 800 °C.

Thermal decomposition of hydroxide precursor

Mass loss related to the different steps of decomposition, as well as the composition of the corresponding phases are presented in the Table 1.

The thermal decomposition of the hydroxide precursor up to 800 °C exhibited three endothermic process stages (Fig. 1). According to the TG curve, the thermal decomposition process is characterised by two apparent falls in sample mass in the temperature ranges (200–400 °C) and (620–680 °C), respectively. Each of the falls in the TG curve corresponds to an endothermic peak in the DTA one. No exothermic effects were detected in the DTA curve.

The IR spectrum (Fig. 4) recorded for the sample obtained at 600 °C compared with that observed at 200 °C shows the disappearance of the weak bands corresponding to the hydroxyls at 3400 cm^{-1} and nitrates at 1384 cm^{-1}. This is justified by the first loss of mass of approximately 0.7% as indicated by the TG curve. It also shows the constant presence of bands at 2540, 1800, 1450 and

Scheme 1 Decomposition scheme of oxalate precursor

$$Ca_3Bi_6O_6(C_2O_4)_4(OH)_3NO_3\,0.5H_2O \xrightarrow{35\text{–}75\ ^\circ C} Ca_3Bi_6O_6(C_2O_4)_4(OH)_3NO_3 + 0.5\,H_2O$$

$$Ca_3Bi_6O_6(C_2O_4)_4(OH)_3NO_3 \xrightarrow{200\text{–}260^\circ C} 1.5\,Ca(C_2O_4) + Ca_{1.5}(BiO)_4O(C_2O_4)(OH)_3 + (BiO)_2(C_2O_4) + NO_2 + CO_2$$

$$(BiO)_2(C_2O_4) \xrightarrow{260\text{–}290\ ^\circ C} (BiO)_2CO_3 + CO$$

$$Ca_{1.5}(BiO)_4O(C_2O_4)(OH)_3 \xrightarrow{290\text{–}390\ ^\circ C} 2\,Bi_2O_3 + 1.5\,CaO + CO + CO_2 + 1.5\,H_2O$$

$$1.5\,Ca(C_2O_4) + (BiO)_2CO_3 \xrightarrow{390\text{–}490\ ^\circ C} 1.5\,CaCO_3 + 1.5\,CO + Bi_2O_3 + CO_2$$

$$3\,Bi_2O_3 + 1.5\,CaO \xrightarrow{390\text{–}490\ ^\circ C} 3.75\,Bi_{1.6}Ca_{0.4}O_{2.8}$$

$$3.75\,Bi_{1.6}Ca_{0.4}O_{2.8} + 1.5\,CaCO_3 \xrightarrow{490\text{–}770\ ^\circ C} 3\,CaBi_2O_4 + 1.5\,CO_2$$

875 cm^{-1}, which are similar to those of calcium carbonate [60], present in the form of impurity and formed from the absorption of CO_2 from the air during the synthesis of the precursor.

The X-ray diffractogram and the IR spectrum recorded for the sample obtained at 700 °C confirm the existence of the α-Bi_2O_3 oxide (JCPDS No. 71-0465) and solid solution as impurity of nature $\beta_2Bi_{2(1-x)}Ca_{(x)}O_{(3-2x)}$ obtained by the reaction of carbonate with a corresponding quantity of oxide. A visibly strong endothermic peak occurred at 740 °C without any accompaniment in weight loss may be attributed to the transitions of the phases of the monoclinic α-Bi_2O_3 to cubic δ-Bi_2O_3 and of the solid solution $\beta_2Bi_{2(1-x)}Ca_{(x)}O_{(3-2x)}$ to $\beta_1Bi_{2(1-x)}Ca_{(x)}O_{(3-x)}$.

The IR spectrum illustrates successive intense bands located at 343, 347, 351, 355, 359, 363, 371, 420, 497 and 538 cm^{-1}, which are assigned to the vibration of Bi–O bonds in the α-Bi_2O_3 compound. One observes that when there is a weak substitution of the Bi by Ca, the case of $\beta_2Bi_{2(1-x)}Ca_{(x)}O_{(3-x)}$ (IR at 800 °C), the intensities of the bands situated at 351 and 355 cm^{-1} decrease and constitute themselves like a shouldering. The same behaviour of these two bands is found in $CaBi_2O_4$ (IR at 800 °C) in the presence of similar peaks at 347, 359 and 371 cm^{-1} and with a displacement of the others at 339, 512 and 549 cm^{-1}.

According to the studies of FTIR and XRD, it revealed that a precipitate obtained without oxalate and dried in an oven is composed mainly of the α-Bi_2O_3 oxide.

The SEM micrographs of calcium bismuth oxides powders prepared from oxalate and hydroxide coprecipitation and calcined at temperature of 800 and 700 °C, respectively, are shown in Fig. 5.

Particles morphology of calcined powder (700 °C for 6 h) of $CaBi_2O_4$ prepared by oxalate process is irregular in shape and has varying dimensions. A good fraction of small-sized particles with dimension of around 300 nm is perceptible. The crystallite size calculated from Scherer's

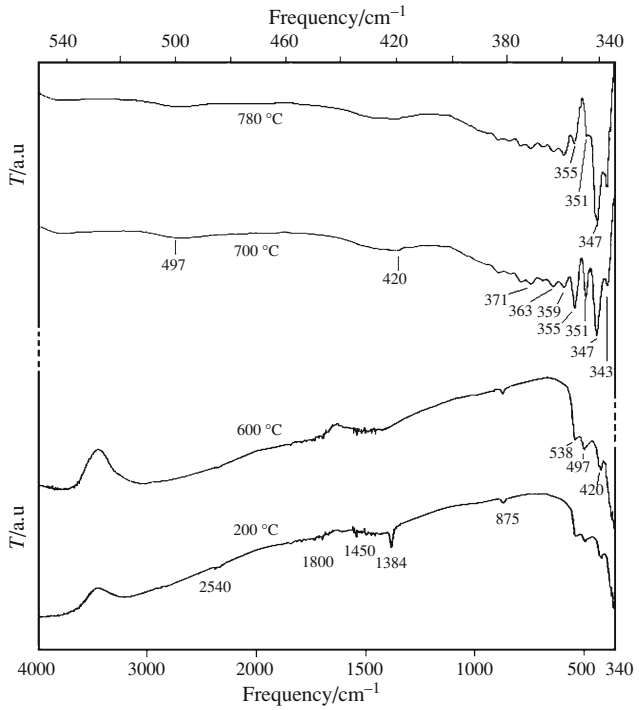

Fig. 4 IRTF spectra of the hydroxide precursor heat-treated at various temperatures

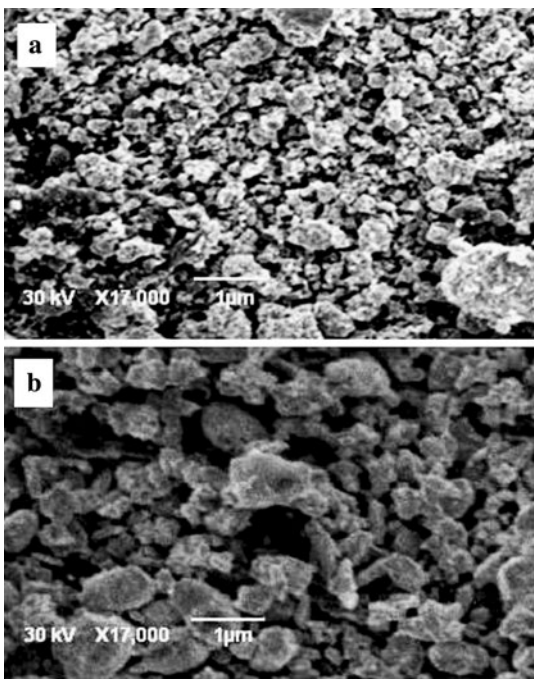

Fig. 5 SEM micrographs of $CaBi_2O_4$ (**a**) and α-Bi_2O_3 (**b**)

equation $D = K\lambda/\beta\cos\theta$, where D is the average size of the crystallites, $K = 0.9$ assuming particles are spherical, λ, the wavelength of X-ray radiation, β, the full width at half maximum of the diffracted peak and θ, the angle of diffraction is 400 nm.

On the other hand, SEM micrograph of the oxide obtained by coprecipitation using only the diethylamine without the oxalic acid, shows that the crystallite sizes are more uniform and larger, in the micrometre range, than those watched previously.

Conclusions

Fine particles of $CaBiO_4$ were successfully prepared by coprecipitation at pH 11 by using oxalic acid and diethylamine with subsequent calcinations at 800 °C. The solid solution $Ca_{0.2}Bi_{0.8}O_{1.4}$ is formed initially from 390 °C, which leads, while reacting with $CaCO_3$ to the formation of $CaBi_2O_4$ with average particle size of 400 nm. On the other hand, without the presence of oxalic precipitant, α-Bi_2O_3 was formed fruitfully after heating the hydroxide precipitate in the drying oven at 80 °C, and there is a minor quantity of calcium which precipitated in the form of $CaCO_3$ and which conduct to the formation of the solid solution $\beta_2Bi_{2(1-x)}Ca_{(x)}O_{(3-2x)}$ from 620 °C as impurity. This result confirms that calcium forms a bimetallic complex with bismuth in the oxalate precursor with a proposed formula: $Ca_3[Bi_6O_6(C_2O_4)_4(OH)_3NO_3]0.5H_2O$.

References

1. Durrani SK, Qureshi AH, Qayyum S, Arif M. Development of superconducting phases in BSCCO and Ba-BSCCO by sol spray process. J Therm Anal Calorim. 2009;95:87–91.
2. Arshad M, Qureshi AH, Masud K, Qazi NK. Production of BSCCO bulk high T_c superconductors by sol-gel method and their characterization by FTIR and XRD techniques. J Therm Anal Calorim. 2007;89:595–600.
3. Ono T, Utsumi K, Tsukamoto S, Tamaru H, Kataoka M, Noguchi F. Roles of bulk γ(L)-Bi_2MoO_6 and surface β-$Bi_2Mo_2O_9$ in the selective catalytic oxidation of C_3H_6. J Mol Catal. 2010;318:94–100.
4. He Y, Wu Y, Yi X, Weng W, Wan H. Promotive effect of Bi component on propane partial oxidation over $MoBiTeO_x/SiO_2$ catalysts. J Mol Catal. 2010;331:1–6.
5. Zheng Y, Duan F, Chen M, Xie Y. Synthetic $Bi_2O_2CO_3$ nanostructures: novel photocatalyst with controlled special surface exposed. J Mol Catal. 2010;317:34–40.
6. Liu Z, Qi Y, Lu C. High efficient ultraviolet photocatalytic activity of $BiFeO_3$ nanoparticles synthesized by a chemical coprecipitation process. J Mater Sci Mater Electron. 2010;21:380–4.
7. van der Linden EG, Luiz Fernando BM, Eloisa Medeiros M. Evaluation of synthetic routes to pigmentary grade bismuth vanadate. Dyes Pigm. 2011;90:36–40.
8. Šulcová P, Trojan M. Thermal analysis of the Bi_2O_3-Y_2O_3-ZrO_2 pigments. J Therm Anal Calorim. 2008;93:795–8.
9. Becchetti FD, Lister PM, Thorn CE. Bismuth germanate scintillator as a fast high-energy ion detector. Nucl Instrum Methods Phys Res. 1984;225:280–2.
10. de Jesus FAA, da Silva RS, Macedo ZS. Synthesis of $Bi_4Ge_3O_{12}$ ceramic scintillators by the polymeric precursor method. J Therm Anal Calorim. 2010;100:537–41.
11. Poghossian AS, Abovian HV, Avakian PB, Mkrtchian SH, Haroutunian VM. Bismuth ferrites: new materials for semiconductor gas sensors. Sens Actuators B Chem. 1991;4:545–9.
12. Shuk P, Wiemhöfer HD, Guth U, Göpel W, Greenblatt M. Oxide ion conducting solid electrolytes based on Bi_2O_3. Solid State Ionics. 1996;89:179–96.
13. Turkoglu O, Belenli I. Electrical conductivity of g-Bi_2O_3-V_2O_5 solid solution. J Therm Anal Calorim. 2003;73:1001–12.
14. Horn W, Földvari I, Denz C. Holographic data storage in photorefractive bismuth tellurite. J Phys D Appl Phys. 2008. doi: 10.1088/0022-3727/41/22/224006.
15. Conflant P, Bovin JC, Thomas D. Le Diagramme des Phases Solides du Systeme Bi_2O_3-CaO. J Solid State Chem. 1976;18:133–40.
16. Roth RS, Hwang NM, Rawn CJ, Burton BP, Ritter JJ. Phase equilibria in the systems CaO–CuO and CaO–Bi_2O_3. J Am Ceram Soc. 1991;74:2148–51.
17. Vstavskaya EY, Zuev AY, Cherepanov VA. The phase diagram of the bismuth-calcium oxide system. Mater Res Bull. 1994;29:1233–8.
18. Hallstedt B, Rissod D, Gaukler LJ. Thermodynamic assessment of the bismuth–calcium–oxygen oxide system. J Am Ceram Soc. 1997;80:2629–36.
19. Ubaldini A, Artini C, Costa GA, Carnasciali MM, Masini R. Synthesis and thermal decomposition of mixed Gd–Nd oxalates. J Therm Anal Calorim. 2008;91:797–803.
20. Maeda H, Tanaka Y, Fukutomi M, Asano T. A new high-T_c oxide superconductor without a rare earth element. Jpn J Appl Phys. 1988;27:209–10.
21. Nielsen KA. Thermal analysis in the research and development of advanced technical ceramics. Thermochim Acta. 1991;175:13–24.
22. Monnereau O, Tortet L, Llewellyn P, Rouquerol F, Vacquier G. Synthesis of Bi_2O_3 by controlled transformation rate thermal analysis: a new route for this oxide? Solid State Ionics. 2003;157:163–9.
23. Kitaguchi H, Shitani F, Egi T, Oda K, Takada J, Osaka A, Miura NY, Ikeda Y, Tanako M. Preparation of the high-Tc phase in the Bi-Pb-Sr-Ca-Cu-O system. Mol Cryst Liq Cryst. 1990;84:129–33.
24. Carp O, Patron L, Marinescu G, Pascu G, Budrugeac P, et al. Copper-iron oxides obtained by thermal decomposition of oxalic coordination compounds. J Therm Anal Calorim. 2003;72:263–70.
25. Deb N. Thermal Investigations of $M[La(C_2O_4)_3]\cdot xH_2O$ (M = Cr(III) and Co(III)). J Therm Anal Calorim. 2002;63:699–712.
26. Marbach G, Stotz S, Klee M, De Vries JWC. Superconductivity in Bi-Sr-Ca-Cu-O bulk samples made by thermal decomposition of metal oxalates. Phys C. 1989;161(1):111–20.
27. Mansori M, Satre P, Breandon C, Roubin M, Sebaoun A. Elaboration et caractérisation de cuprates de bismuth supraconducteurs. Ann Chim. 1993;18:537–47.
28. Shei CY, Liu RS, Chang CT, Wu PT. Coprecipitation process for the preparation of superconductive Bi-Sr-Ca-Cu oxides. Mater Lett. 1990;9:105–8.
29. Marta L, Zaharescu M, Ciontea L, Petrisorc T. Chemical route to the synthesis of superconducting bismuth oxide system. Appl Supercond. 1993;1:677–91.

30. Zhang Y, Fang Z, Muhammed M, Rao KV, Skumryev V, Medelius H, Costa JL. The synthesis of superconducting bismuth compounds via oxalate coprecipitation. Phys C. 1989;157: 108–14.
31. Spencer ND. Alkali-metal-free carbonate coprecipitation: an effective synthetic route to bismuth-based oxide superconductors. Chem Mater. 1990;2:708–12.
32. Zhang Y, Muhammed M, Wang L, Nogues J, Rao KV. Synthesis of superconducting *Pb*/*Sb* doped BiSrCaCuO compounds via oxalate coprecipitation. Mat Chem Phys. 1992;30:153–9.
33. Chiang C, Shei CY, Huang YT, Lee WH, Wu PT. Preparation of high purity 110 K phase in the (Bi, Pb)-Sr-Ca-Cu-O superconductor system using a solution method. Phys C. 1990;170:383–7.
34. Chuanbin M, Zehua D, Lian Z. Modified coprecipitation process of synthesizing Bi-system superconductor precursor powder and its stoichiometry. Sci China. 1996;E39:181–90.
35. Popa M, Totovana A, Popescu L, Dragan N, Zaharescu M. Reactivity of the Bi, Sr, Ca, Cu oxalate powders used in BSCCO preparation. J Eur Ceram Soc. 1998;18:1265–71.
36. Nakamoto K. IR spectra of inorganic and coordination compounds. 2nd ed. New York: Wiley-Interscience; 1970.
37. Reddy VB, Mehrotra PN. IR and thermal studies on lanthanum zirconyl oxalate. J Therm Anal Calorim. 1981;21:21–6.
38. Nissen DA. The thermal decomposition of plutonium (IV) oxalate hexahydrate. J Therm Anal Calorim. 1980;18:99–109.
39. Balboul BAA, El-Roudi AM, Samir E, Othman AG. Non-isothermal studies of the decomposition course of lanthanum oxalate decahydrate. Thermochim Acta. 2002;387:109–14.
40. Mehring M. From molecules to bismuth oxide-based materials: potential homo- and heterometallic precursors and model compounds. Cood Chem Rev. 2007;251:974–1006.
41. Yang N, Sun H. Biocoordination chemistry of bismuth: recent advances. Cood Chem Rev. 2007;251:2354–66.
42. Suzuki H, Matano Y. Organobismuth chemistry. Amsterdam: Elsevier; 2001.
43. Luckay R, Cukrowski I, Mashishi J, Reibenspies JH, Bond AH, Rogers RD, Hancock RD. Synthesis, stability and structure of the complex of bismuth(III) with the nitrogen-donor macrocycle 1,4,7,10 tetraazacyclododecane. The role of the lone pair on bismuth(III) and lead (II) in determining co-ordination geometry. J Chem Soc Dalton Trans. 1997;26:901–8.
44. Stavila V, Davidovich RL, Gulea A, Whirmire KH. Bismuth(III) complexes with aminopolycarboxylate and polyaminopolycarboxylate ligands: chemistry and structure. Coord Chem Rev. 2006;250:2782–810.
45. Mehring M, Mansfeld D, Paalasmaa S, Schürmann M. Polynuclear bismuth-oxo clusters: insight into the formation process of a metal oxide. Chem Eur J. 2006;12:1767–81.
46. Mansfeld D, Mehring M, Schürmann M. From a monomeric bismuth silanolate to a molecular bismuth oxo cluster: $[Bi_{22}O_{26}(OSiMe_2tBu)_{14}]$. Angew Chem Int Ed. 2005;44:245–9.
47. Tytko KH. Isopolyoxokationen—Metallkationen in wäßriger Lösung. Chem unserer Zeit. 1979;13:184–94.
48. Lazarini F. The crystal structure of a bismuth basic nitrate, $[Bi_6O_5(OH)_3](NO_3)_3.3H_2O$. Acta Crystallogr B. 1978;34:3169–73.
49. Lazarini F. Bismuth basic nitrate, $[Bi_6(H_2O)(NO_3)O_4(OH)_4](NO_3)_5$. Acta Crystallogr B. 1979;35:448–50.
50. Henry N, Mentre O, Abraham F, MacLean EJ, Roussel P. Polycationic disorder in $[Bi_6O_4(OH)_4](NO_3)_6$: structure determination using synchrotron radiation and microcrystal X-ray diffraction. J Solid State Chem. 2006;179:3087–94.
51. Christensen AN, Chevallier MA, Skibsted J, Iversen BB. Synthesis and characterization of basic bismuth(III) nitrates. J Chem Soc Dalton Trans. 2000;29:265–70.
52. Sundvall B. Crystal and molecular structure of tetraoxotetrahydroxobismuth(III) nitrate monohydrate, $Bi_6O_4(HO)_4(NO_3)_6.H_2O$. Acta Chem Scand A. 1979;33:219–24.
53. Asato E, Katsura K, Mikuriya M, Fujii T, Reedijk J. Isolation of a unique hexanuclear $[Bi_6O_4OH(cit)_3(H_2O)_3]^{3-}$ cluster from the bismuth-containing ulcer healing agent "colloidal bismuth subcitrate (CBS)". Chem Lett. 1992;21:1967–70.
54. Logvinenko V, Mikhailov K, Yu Y. The kinetics of thermal decomposition of bismuth oxohydroxolaurate. J Therm Anal Calorim. 2007;88:47–9.
55. Sillèn LG. Die Kristallstruktur einiger Strontium—Wismutoxyhalogenide $[SrBi_3O_4Cl_3$, $SrBiO_2Br$, $SrBi_2O_3Br_2$ und $SrBi_3O_4Br_3]$. Z Anorg Allg Chem. 1941;246:115–30.
56. Missyul' AB, Khairullina EM, Zvereva IA. Synthesis of the Aurivillius phases $Bi_2LnTaTiO_9$ (Ln = La, Nd, Sm, Gd). Glass Phys Chem. 2010;36:247–50.
57. Greaves C, Blower SK. Structural relationships between $Bi_2O_2CO_3$ and β-Bi_2O_3. Mater Res Bull. 1988;23:1001–8.
58. Taylor P, Sunder S, Lopata VJ. Structure, spectra, and stability of solid bismuth carbonates. Can J Chem. 1984;62:2863–73.
59. Aurivillius B. X-ray studies of bismuth oxide acetate, $CH_3COO.OBi$ and related compounds. Acta Chem Scand. 1955;9:1213–8.
60. Srivastava A, Gunjikar VG, Sinha APB. Thermoanalytical studies of zinc citrate, bismuth citrate and calcium citrate. Thermochim Acta. 1987;117:201–17.